



Общероссийский математический портал

V. G. Shemanin, E. V. Kolpakova, A. B. Atkarskaya, O. V. Mkrtychev, SiO₂ barrier layer influence on the glass composites with oxide nano films laser ablation destruction,

Наносистемы: физика, химия, математика, 2019, том 10, выпуск 6, 632–636

<https://www.mathnet.ru/eng/nano478>

Использование Общероссийского математического портала Math-Net.Ru подразумевает, что вы прочитали и согласны с пользовательским соглашением

<https://www.mathnet.ru/rus/agreement>

Параметры загрузки:

IP: 18.97.14.84

24 мая 2025 г., 15:06:56



SiO₂ barrier layer influence on the glass composites with oxide nano films laser ablation destruction

V. G. Shemanin¹, E. V. Kolpakova¹, A. B. Atkarskaya², O. V. Mkrtichev²

¹Novorossiysk Polytechnic Institute of Kuban State Technological University,
Karla Marksa street, 20, Novorossiysk, 353900, Russia

²Belgorod State Technological University named after V. G. Shukhov,
Novorossiysk branch, Myskhakskoe shosse, 75, Novorossiysk, 353919, Russia

vshemanin@yandex.ru, evge.kolpakova@yandex.ru, atkarsk06@mail.ru, oleg214@ya.ru

PACS 65.80.-g, 68.35.bj, 68.60.-p, 68.90.+g

DOI 10.17586/2220-8054-2019-10-6-632-636

This study concerns the composites optical characteristics dependence on the chemical composition of the oxide nanofilms from TiO₂–Me_xO_y and on the existence of a SiO₂ barrier layer. The laser ablation destruction threshold energy density values decrease with the light transmission growth in the visible range of the composites for one- and double-layer nanofilms. These properties measurement results dependences for the composites with one- and double-layer nanofilms can be connected with various structure and composition of the complexes which were formed in the films.

Keywords: glass composites, nano film, laser ablation, threshold energy density, light transmission.

Received: 5 July 2018

Revised: 25 November 2019

1. Introduction

The nano dimensional oxide films using for the efficient change in the instrumental glass details properties allows one to considerably expand the range of application for modified glass composites [1–5]. Nano films are applied to change of the optical characteristics – the increasing in the light transmission by the optical details or giving of the reflecting properties [1, 4] to them. Such a film is obtained by the sol-gel technology including the contact of a film-forming solution with a glass substrate [3, 6–10]. The glass surface becomes covered by the oxide one- or multilayer nano films in this case. And, besides the basic functional purpose, the nano film will follow up provide the resistance to the surrounding medium influence [2, 11].

The influence of a SiO₂ barrier layer on the laser ablation destruction threshold energy density of the glass composites with the bicomponent oxide nano films of the TiO₂–Me_xO_y structure was studied after [3, 4]. The threshold density dependence on the composite other optical parameters – the light transmittance in the visible range, reflectivity coefficient at the 1064 nm laser radiation wavelength, an refractive index and a layer thickness were also investigated in detail.

This goal of these studies is the composites optical characteristics dependence on the chemical composition of the bicomponent oxide nano films from TiO₂–Me_xO_y and on the existence of a SiO₂ barrier layer. The knowledge of such a composite's properties will allow creation of new materials for nanophotonics with the new linear and non-linear optical properties.

2. Experimental samples and methods

The glass composites samples with the bicomponent oxide nanofilms with the structure of TiO₂–Me_xO_y have been received by the sol-gel technology. The alloying Me_xO_y oxide amount was 2 or 10 mass %. Starting materials were the titanium tetraethoxide and the copper, tin, zinc, cadmium and iron chlorides. The oxides sum mass content in the film-forming sol have been of 5 mass. %. The films were drawn on the float-glass substrate by the dipping method and the samples withdrawal rate from the sol was of 3.8 mm/s. The heat treatment in the microwave oven – the furnace was made within 30 minutes. The thickness, refractive index, film reflectivity have been measured by the Horiba Jobin Yvon type spectra ellipsometer as in [12] and the samples light transmittance by a FSD-8 type micro spectrometer (NCFO RAS).

The composites laser ablation destruction under the pulse laser radiation influence were studied at the experimental layout described in [10] and by the technique given in [4]. The YAG-Nd laser generated the radiation pulses at the 1064 nm wavelength of the 20 ns time duration and the pulse energy up to 0.15 J in the mode locking regime. The laser radiation was focused by the lens objective on the composite sample surface. The breakdown phenomenon was fixed on the existence of the laser plasma plume characteristic luminescence and was recorded by the FSD-8 type micro

spectrometer with the fiber input. The laser pulse energy density changing in the range from 0.1 to 180 J/cm² was reached by the choice of this lens focal distance and the laser radiation weakening by the NS type calibrated neutral light filters. The photodiode with the glass light filter IKS-1 was used for the laser pulse energy monitoring. Management of duties of the spectrometer operation regimes controlling and the observed data processing were carried out in PC.

3. Experimental results

The film's thickness, refractive index and reflection coefficient at the 1064 nm wavelength have been measured by the Uvisel 2 type Horiba Jobin Yvon spectra ellipsometer. The experimental results were treated statistically and exhibited in Fig. 1 and Fig. 2.

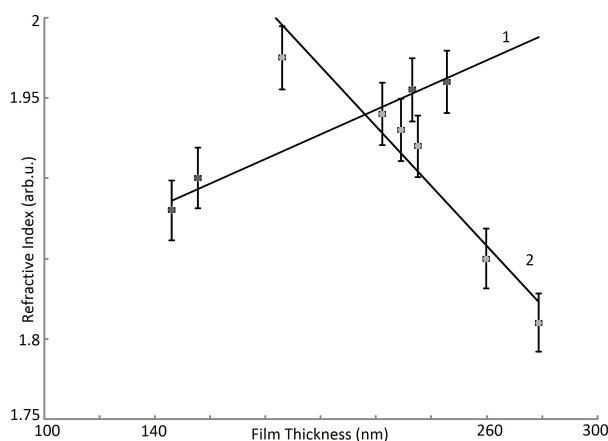


FIG. 1. The plot of the film refractive index n dependence on the film h thickness: 1 – the drawing speed of 3.8 mm/s, 2 – the drawing speed of 5.8 mm/s

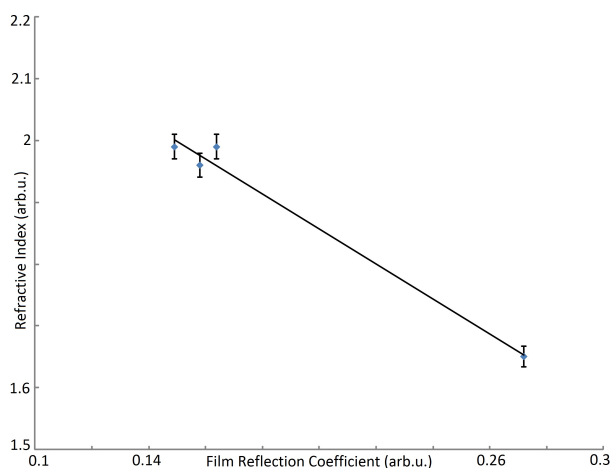


FIG. 2. The plot of the film refractive index n dependence on the film reflection coefficient at the 1064 nm wavelength and the drawing speed of 5.8 mm/s

The experimental straight lines of the trends in Fig. 1 shows that the drawing speed has significant effect on the film refractive index dependence on its thickness. This dependence is due to the sol particles packing density in a layer increases with the drawing speed from the sol particles diameter decreasing. Its increasing, probably, is connected with the influence of the light dispersion which is more, than more the film thickness for the film refractive index dependence on its thickness [12].

The films refractive index reduction with its reflection coefficient at the 1064 nm wavelength growth in Fig. 2 is explained by the same dispersion in the growth bulk of the film and the smaller size of sol particles and their more dense packing in the film layer [6].

At the next stage, the calibration experiments were executed at the target from a clear substrate – float glass and the threshold energy density at the breakdown probability of 0.5 was equal $F_{bn} = 143 \text{ J/cm}^2$. It is necessary to make not less than 30 measurements at the given laser radiation pulse energy to generate the laser ablation destruction probability curve and to measure the ratio of the breakdown events number at the target surface to the total radiation pulses number. All range of the breakdown probability values from 1 to 0 were sequentially obtained over by changing the pulse energy value and repeating this process. The exact interpretation of this probability curve is important for the precise determination of the threshold energy density value of the composites laser destruction with the probability of 0.5. The calibration procedure allowed us to develop the threshold energy density measurement algorithm including the precise positioning and movement of the target about the laser beam.

Then, the breakdown probabilities curves for all samples, as well as in [9], have been obtained. The threshold energy density values of F_{bn} for all composites from these dependence at the probability level of $p = 0.5$ have been determined and such values of the laser ablation destruction threshold energy density of F_{bn} dependences on the composites light transmission in the visible range of T for the drawing speed of 3.8 mm/s for the one- and double-layer nanofilms are given in Fig. 3.

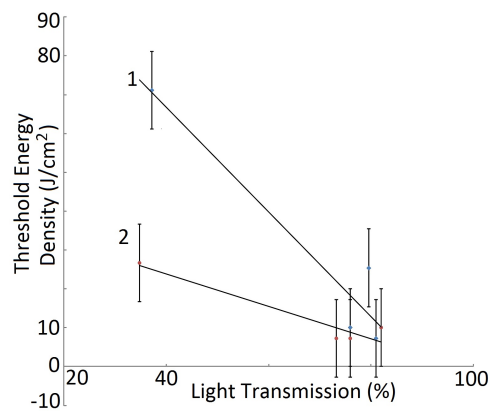


FIG. 3. The plots of the laser ablation destruction threshold energy density of F_{bn} dependence on the composites light transmission in the visible range of T . The line 1 – a one-layer film, line 2 – double-layers one. Drawing speed – 3.8 mm/s

The laser ablation threshold energy density values decrease with increased light transmission as it appears from Fig. 3. It is possible to explain by the light losses decreasing in the composites volume due to the reflection and scattering on the particles in the film volume. This leads to decrease in the laser radiation ratio reflected at the composite surface with the high reflectivity coefficient and then the ablation destruction effectiveness increases.

It is also confirmed by the analysis of the laser ablation destruction threshold energy density of F_{bn} dependence on the reflectivity coefficient at the 1064 nm laser radiation wavelength of R_{1064} in Fig. 4.



FIG. 4. The plots of the laser ablation destruction threshold energy density of F_{bn} dependence on the composites light transmission in the visible range of T . The line 1 – a one-layer film, line 2 – double-layers one. Drawing speed – 3.8 mm/s

It has been derived that the threshold energy density value increases with higher reflectivity coefficient values, which is explained by the ratio of the laser radiation reflected energy at the film surface increasing. The reflectivity coefficient decreasing in the double-layer films is bound to the film refractive index lowering due to the SiO₂ barrier layer as well as in [12].

The threshold energy density of the laser ablation destruction F_{bn} dependences on the film h thickness for all composites samples with single-layer film and the drawing speeds of 3.8 mm/s are given in Fig. 5.

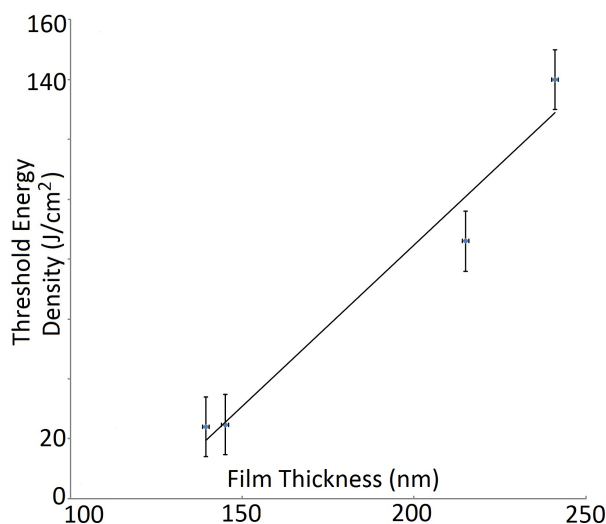


FIG. 5. The plot of the laser ablation destruction threshold energy density of F_{bn} dependence on the film h thickness. The drawing speed is 3.8 mm/s

As appears from a straight line in Fig. 5, the threshold energy density value is higher, than more thickness of the film. At the same time, this threshold energy density value for the double-layer film remains almost invariable with an accuracy of our measurements in this range of the films thickness.

As a result, the studied parameter properties of the composites with single-layer nanofilm changed in the following limits: the threshold energy density of the laser ablation destruction F_{bn} of 6.6 – 143 J/cm², light transmittance in the visible range of T of 36.8 – 84.3 %; film thickness h is 144.8 – 272.3 nm, an refractive index of n 1.6496 – 1.9926, and R_{1064} reflectivity coefficient at the 1064 nm wavelength – 0.041 – 0.286 arb. units. And for composites with double-layer film they changed in the following limits: the threshold energy density F_{bn} of 6.6 – 32.4 J/cm², light transmittance in the visible range of T of 34.8 – 85.8 %; film thickness h is 133.3 – 221.8 nm, an refractive index of n 1.6358 – 1.9952, and R_{1064} reflectivity coefficient – 0.042 – 0.184 arb. units.

Such the difference of these properties measurements result can be connected with various structure and composition of the complexes which are formed in these films [3, 4, 12].

4. Conclusion

The laser ablation destruction threshold energy density values decrease with the light transmission growth in the visible range of the composites for single- and double-layer nanofilms. This is explained by the decreasing in the light losses of the reflecting component.

The analysis of the threshold energy density of the laser ablation destruction dependence on the reflectivity coefficient at the 1064 nm laser radiation wavelength confirms this conclusion, and the reflectivity decreasing in the double-layer films is bound to the film's refractive index decrease due to the SiO₂ barrier layer.

The value of threshold energy density is higher, with increased thickness of the film. At the same time this threshold density value for a double-layer film, with the accuracy our measurements, remains almost invariable in this range of the film thickness.

In general, such difference of these properties measurement results for the composites with one- and double-layer nanofilms can be connected with various structure and composition of the complexes which were formed in the films.

Acknowledgements

This work was partially supported by the Basic part of State assignment of the Ministry of Education and Science of the Russian Federation, project No. 5.7721.2017/BC.

References

- [1] Magnozzi M., Terreni S., et al. Optical properties of amorphous SiO₂-TiO₂ multi-nanolayered coatings for 1064-nm mirror technology. *Opt. Mat.*, 2018, **75**, P. 94–101.
- [2] Sung Y., Malay R.E., et al. Anti-reflective coating with a conductive indium tin oxide layer on flexible glass substrates. *Appl. Opt.*, 2018, **57** (9), P. 2202–2207.
- [3] Vytykáčová S., Mrázek J., et al. Sol-gel route to highly transparent (Ho_{0.05}Y_{0.95})₂Ti₂O₇ thin films for active optical components operating at 2 μm. *Opt. Mat.*, 2018, **78**, P. 415–420.
- [4] Shemanin V.G., Atkarskaya A.B. Breakdown of Glass Composites with a TiO₂ Nanodimensional Coating by Laser Ablation. *Technical Phys.*, 2016, **86** (2), P. 140–142.
- [5] Lyubas G.A. Generation of laser radiation by nanostructured solid active elements with selective optical nanoresonators formed in nanoporous aluminum oxide films. *Nanosystems: Physics, Chemistry, Mathematics*, 2017, **8** (6), P. 793–797.
- [6] Ottermann C.R., Bange K. Correlation between the density of TiO films and their properties. *Thin Sol. Films*, 1996, **286** (1–2), P. 32–34.
- [7] Janicki V., Sancho-Parramon J., et al. Optical characterization of hybrid antireflective coatings using spectrophotometric and ellipsometric measurements. *Appl. Opt.*, 2007, **46** (24), P. 6084–6091.
- [8] Atkarskaya A.B., Mkrtychev O.V., Privalov V.E., Shemanin V.G. Laser ablation of the glass nanocomposites studies. *Opt. Mem. Neural Networks*, 2014, **23** (4), P. 265–270.
- [9] Cai Q.-Y., Zheng Y.-X., et al. Evolution of optical constants of silicon dioxide on silicon from ultrathin films to thick films. *J. Phys. D, Appl. Phys.*, 2010, **43**, 445302.
- [10] Melikhov I.F., Popov I.Yu. Asymptotic analysis of thin viscous plate model. *Nanosystems: Physics, Chemistry, Mathematics*, 2018, **9** (4), P. 447–456.
- [11] Privalov V.E., Shemanin V.G., Mkrtychev O.V. Method of assessing the optical resistance of an irradiated surface under laser ablation. *Meas. Tech.*, 2018, **61** (7), P. 694–698.
- [12] Atkarskaya A.B., Shemanin V.G. Influence of the Interaction of Components in a Transient Layer of Oxide Film Glass Substrate on Properties of the Composite Material. *Glass Physics and Chemistry*, 2015, **41** (5), P. 515–521.